Vertical Winds in the Southern Auroral Thermosphere Observed Concurrently at E- and F-region Altitudes

Callum Anderson[1], Mark Conde[1], Theo Davies[2], Peter Dyson[2], Mike Kosch[3]
1) Geophysical Institute, University of Alaska Fairbanks, USA . 2) Department of Physics, Latrobe University, Australia.
3) Department of Physics, Lancaster University, UK.

1. ABSTRACT

Vertical winds are a poorly understood component of the upper atmospheric circulation. Vertical hydrostatic stability, coupled with the strong positive temperature gradient that exists throughout the region, should effectively restrict the motion of air parcels normal to constant pressure surfaces (or at least turn these motions into oscillatory ones). However, observations of fast (50-100 ms^{-1}) vertical winds have been reported in the literature. Figure 1, below, shows an example of these large vertical winds, largely confined to northern and southern auroral latitudes, observed by the Dynamics Explorer 2 satellite in 1982.

As a consequence of the difficulties associated with observing vertical atmospheric motions in the upper atmosphere, we have very little knowledge of the horizontal spatial structure of the vertical wind field, and even less of the vertical structure. During 2011, a campaign of bistatic observations was conducted using two Fabry-Perot spectrometers in Antarctica. Both instruments were configured to interleave their observations between E- and F-region altitudes. By combining the data from both instruments, estimates were made of the E-region vertical wind at 4 locations, and the F-region vertical wind at 5 locations (at the higher altitude, there is greater field-of-view overlap), spanning a magnetic latitude range of approximately 4°. Here we present results from that campaign, and demonstrate both the horizontal and vertical structure that was observed.

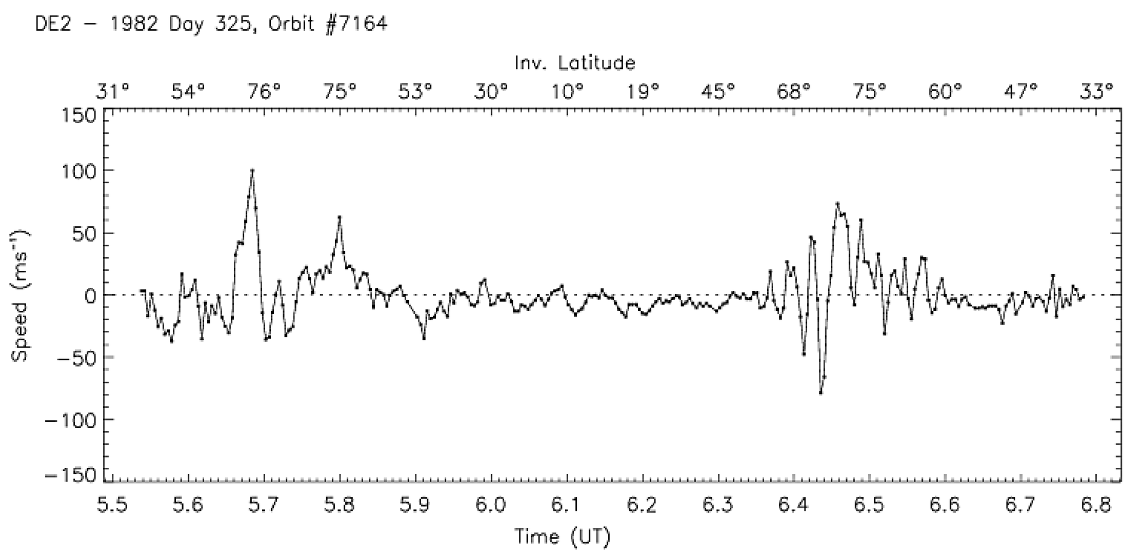

Figure 1: Vertical winds derived from Dynamics Explorer 2 satellite measurements during orbit #7164, 1982.

2. ANALYSIS

In the F-region, where airglow emission height variation is not usually significant, overlapping Mawson-Davis fields-of-view are easily identified. Bistatic winds are then derived in those locations using measurements from both instruments (see Figure 2). In the E-region, the airglow peak emission altitude varies depending on the characteristic energy of the aurora. To identify common-volumes, we do the following:

1. Estimate the 558 nm airglow emission height at each location from Mawson temperature measurements, using the NRLMSISE-00 model to 'look-up' the altitude for a given temperature.
2. Project the Davis line-of-sight until it intersects the inferred emission layer (find the latitude/longitude coordinates of the intersection).
3. Find the Mawson zone closest to that location.

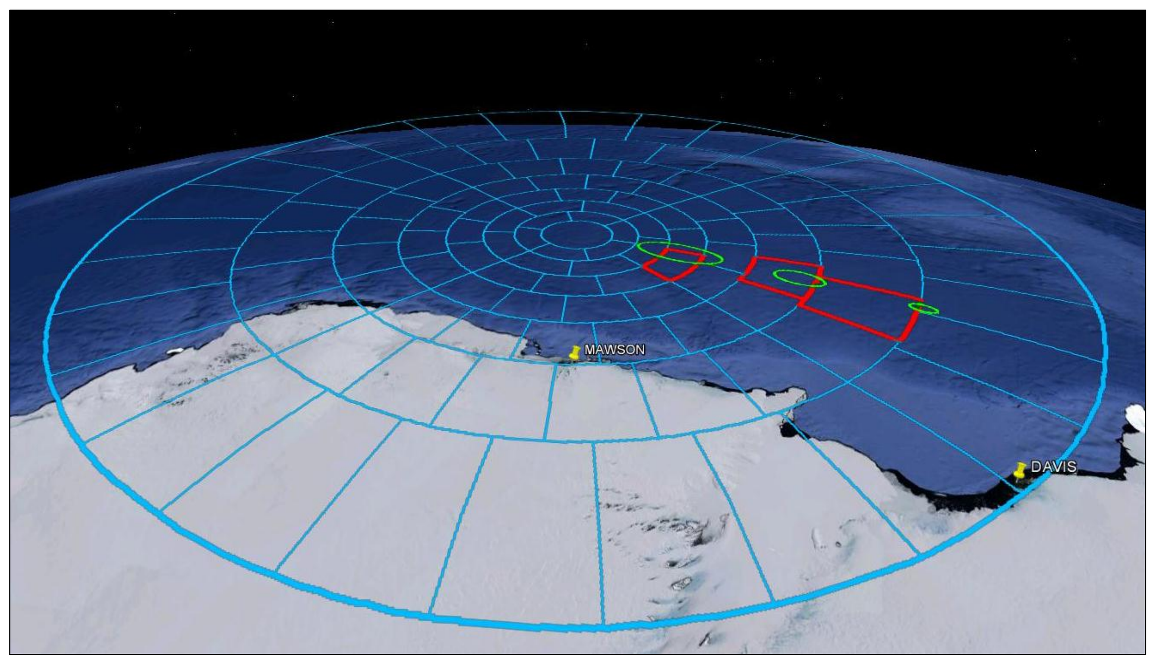

Figure 2: Common-volume (bistatic) locations at F-region altitudes. Green lines show Davis fields-of-view, red lines highlight Mawson viewing zones. Zones are shown with correct perspective at an altitude of 240 km.

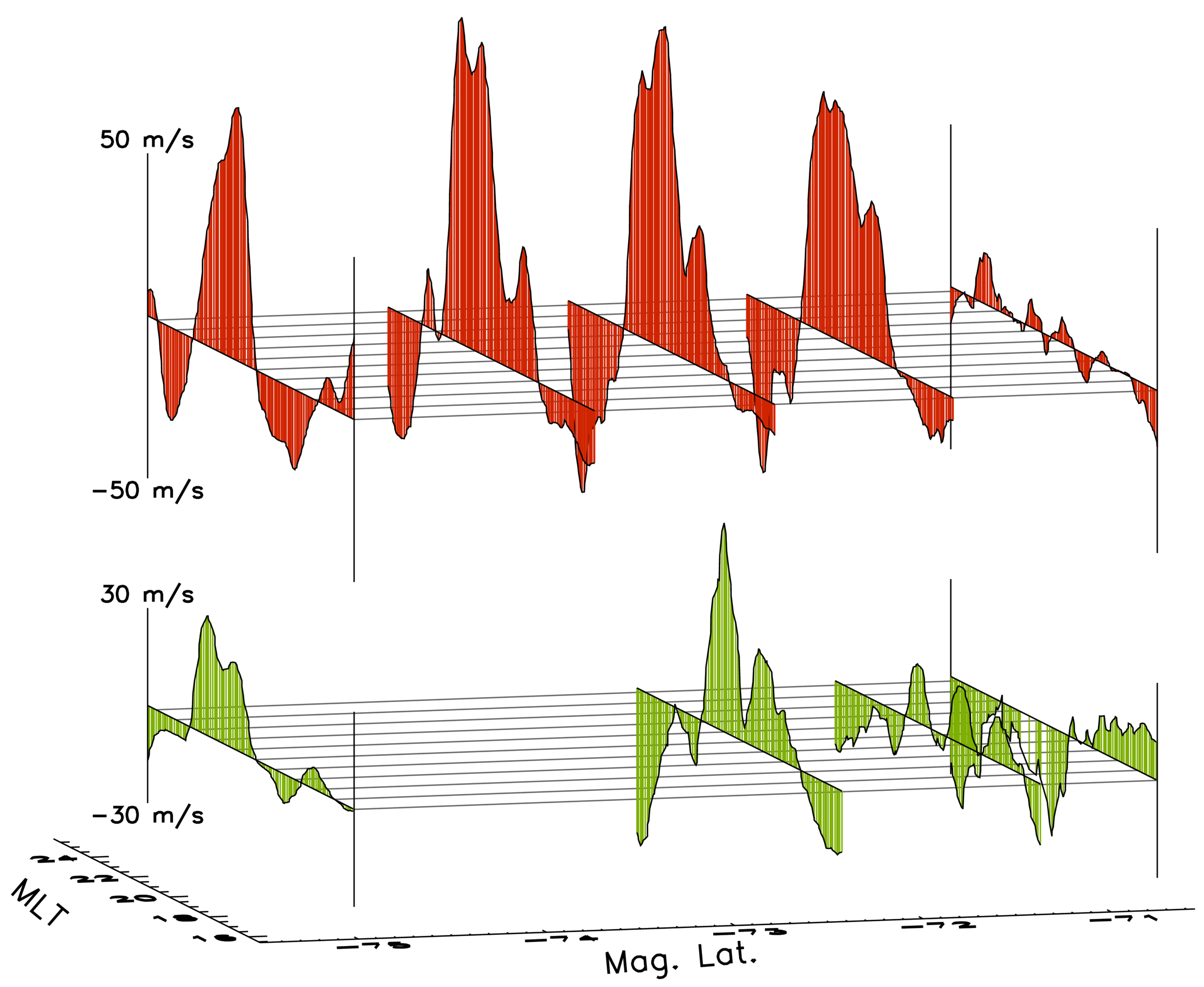

Figure 3: Bistatic vertical winds, in the F-region (red) and E-region (green), measured on day 101, 2011. Note that common-volume locations are defined along the great-circle between the stations, and as the great circle is close to magnetic north-south aligned, volumes are plotted by magnetic latitude.

In a given common-volume, the two-component wind vector has components along the Mawson-Davis great circle, and in the local zenith direction (v_x and v_z respectively). The line-of-sight winds measured from Mawson (v_m) and Davis (v_d) in the common-volume are then given by:

$$\begin{bmatrix} v_m \\ v_d \end{bmatrix} = \begin{bmatrix} m_x & m_z \\ d_x & d_z \end{bmatrix} \begin{bmatrix} v_x \\ v_z \end{bmatrix}$$

where (m_x, m_z) and (d_x, d_z) are the unit vectors along the Mawson and Davis lines-of-sight to the common-volume. In terms of zenith look-angles, the common-volume, two-component wind vector is obtained through inversion:

$$\begin{bmatrix} v_x \\ v_z \end{bmatrix} = \begin{bmatrix} \sin(\theta_m) & \cos(\theta_m) \\ -\sin(\theta_d) & \cos(\theta_d) \end{bmatrix}^{-1} \begin{bmatrix} v_m \\ v_d \end{bmatrix}$$

The vertical wind is then given by v_z, and the horizontal wind along the Mawson-Davis great circle by v_x. An example of derived vertical winds in each common-volume is given in Figure 3.

3. AVERAGE SPATIAL-TEMPORAL STRUCTURE

From the data collected during 2011, 62 days were identified as cloud-free. Averaging over those 62 days provides insight into the average structure of the vertical wind field, in altitude (due to the variable E-region emission height), magnetic latitude (Mawson and Davis are close to magnetic north-south aligned) and in time. Figures 4 and 5, on the right, separate the dataset into E-region (<200 km altitude) and F-region (240 km altitude) observations, and bin the data by magnetic local time and magnetic latitude. There is quite strong correlation displayed between the E- and F-region average vertical winds, in particular upward winds in the early afternoon (1000-1500 MLT) and in the magnetic midnight sector (2000-0100 MLT). The second of these is particularly strong, with average winds of 20 ms^{-1} above Davis, decreasing in magnitude toward Mawson. The very similar temporal structure at both altitudes strongly suggests that the vertical winds are responding to the same geophysical drivers on average.

Figure 6 exploits the variability in the E-region emission altitude to sample the height structure of the vertical wind magnitude. Each data point shows the median vertical wind magnitude in a particular altitude bin. The data suggest a peak magnitude around 140 km altitude. These results in are very recent, and we are currently investigating them in greater detail, in combination with similar data from Alaska, to ascertain what combination of processes might be responsible for this altitude structure.

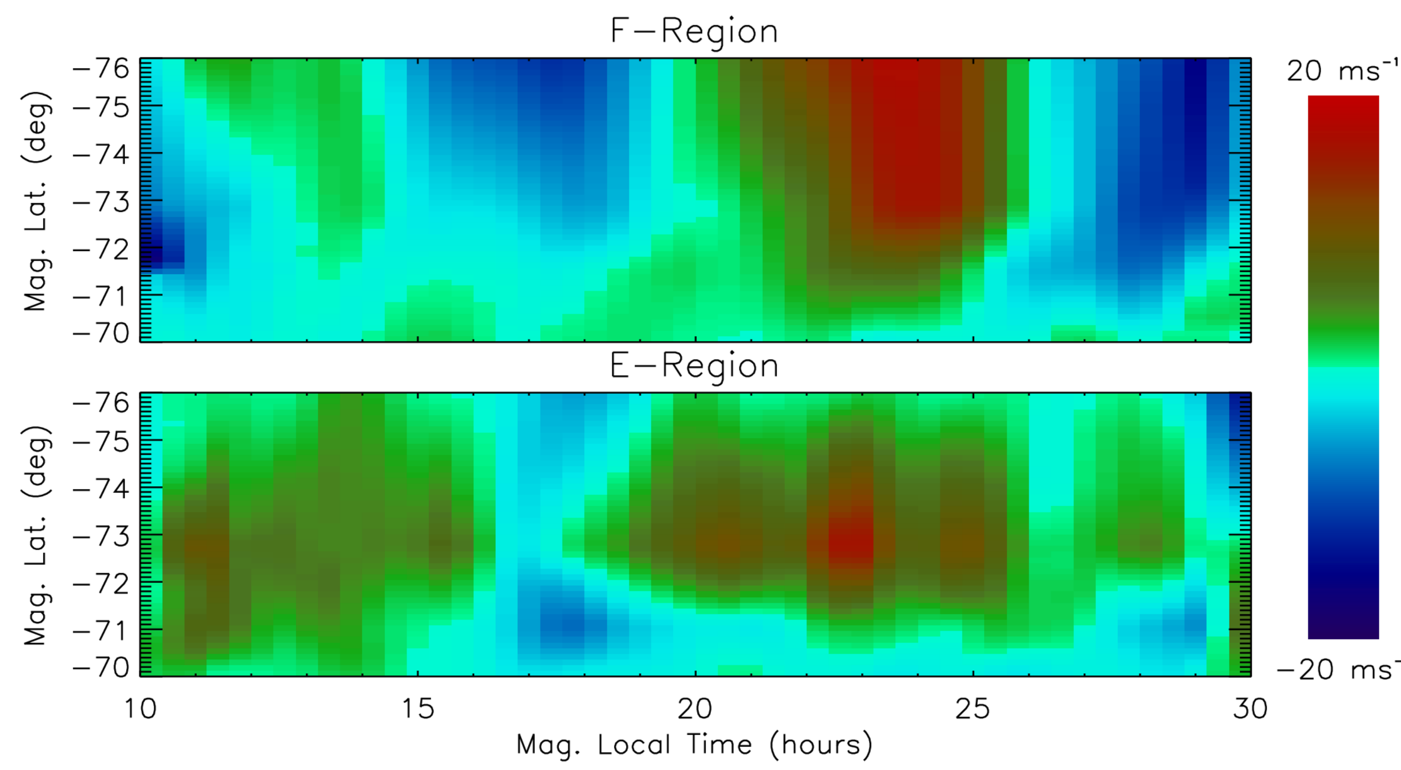

Figure 4: Average vertical winds recorded during the 2011 common-volume campaign. Upper panel shows average F-region vertical wind, lower panel shows E-region vertical wind. Winds are shown as a function of magnetic local time and magnetic latitude (Davis station is at the top of each panel, Mawson at the bottom).

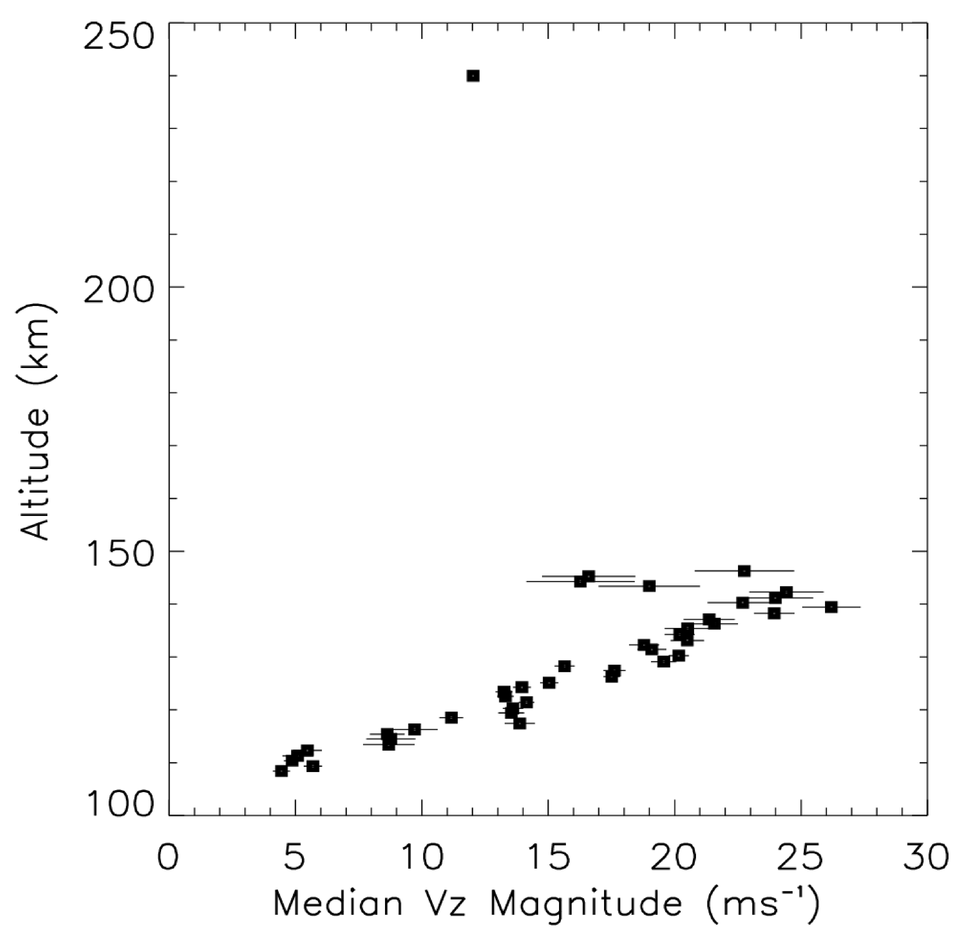

Figure 6: Median vertical wind magnitude as a function of altitude (for bins containing 50+ observations).

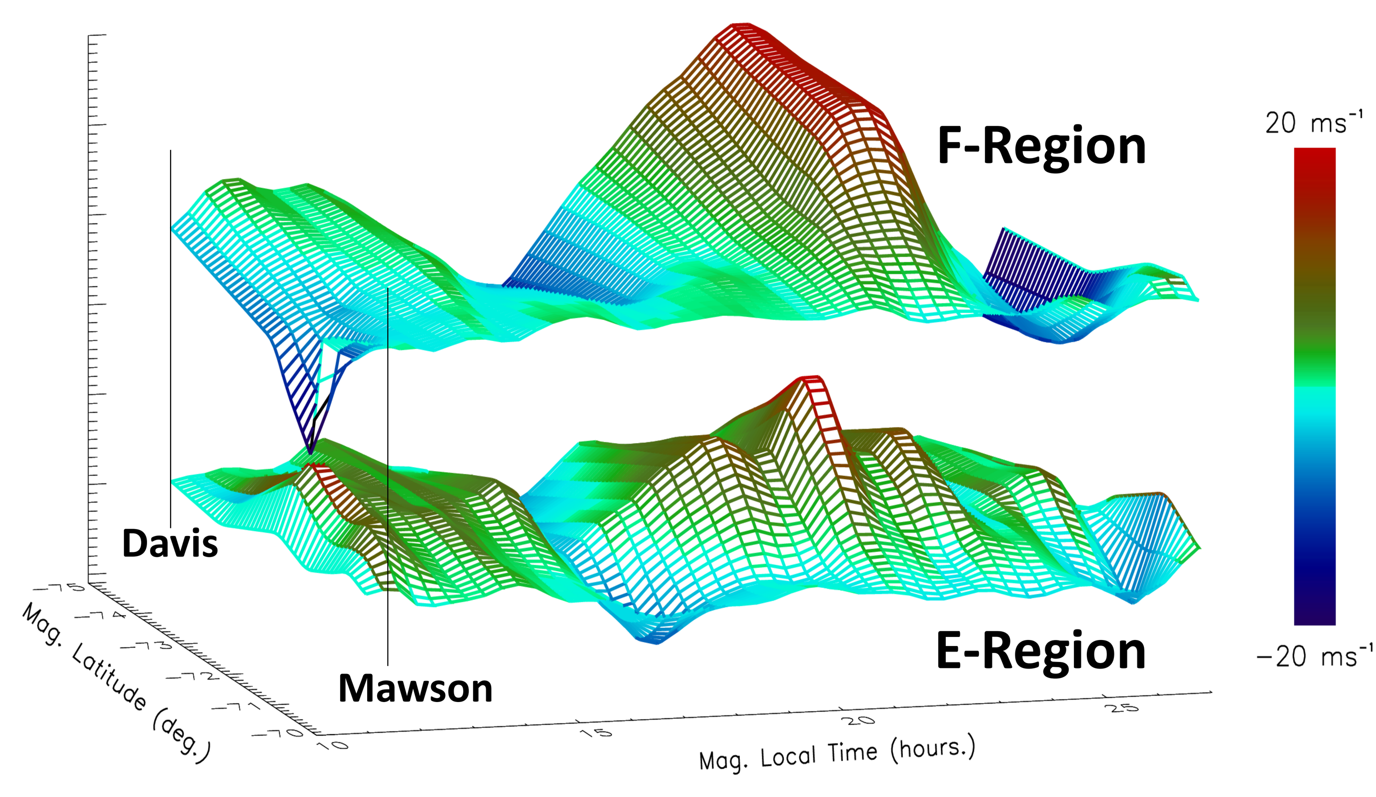

Figure 5: Three-dimensional view of the average vertical wind structure shown in Figure 4.

4. SUMMARY

Vertical winds play a very important role in atmospheric dynamics and transport, because the strongest gradients (e.g. temperature, composition, wind speed) are typically vertical gradients. Thus despite the fact that vertical wind magnitudes are usually small (< 30 ms^{-1}), they can be responsible for disproportionately large local perturbations. At auroral latitudes, horizontal winds are often fast and highly structured (for example wind shears in the presence of auroral arcs are a common feature of the high-latitude F-region wind field). Horizontal winds can take small-scale, local perturbations, driven by vertical winds, and transport them long distances, distorting them ('stretching' them out via shears, for example) as they go. In this way, small-scale processes like vertical winds can have non-negligible impacts on the global-scale system.

Bistatic measurements provide a valuable new dataset for understanding vertical winds. With a single ground-based instrument, vertical winds can only be measured in the local zenith, yielding only single-point measurements. The bistatic technique presented here allows vertical winds to be measured along the line joining the two instruments, at altitudes determined by the airglow emission height profile, thereby resolving vertical wind structure in two dimensions. Despite this being only a small slice of what is a complex, highly variable, three-dimensional scalar field, this is still a great improvement over existing techniques and is providing us with new insights into the way vertical winds are structured both horizontally and vertically.